High Performance Microcrack-based MWCNT-rubber Strain Sensor

Fei Wang
Deparment of Mechanical Engineering, Material Science and Engineering Program
University of Houston
Houston, USA
fwang5@uh.edu

Pengcheng Wang
Deparment of Mechanical Engineering
University of Houston
Houston, USA
pwang13@uh.edu

James Jenkinson
Department of Mechanical Engineering, Materials Science and Engineering Program
University of Houston
Houston, USA
jwjenki2@central.uh.edu

Haowei Zhang
School of Medical Instrument and Food Engineering
University of Shanghai for Science and Technology
Shanghai, China
howiezh@aliyun.com

Fan Zheng*
Department of Engineering Technology
University of Houston
Houston, USA
fanzheng@central.uh.edu

Li Sun*
Department of Mechanical Engineering
University of Houston
Houston, USA
lsun3@central.uh.edu

2021 IEEE 16th Nanotechnology Materials and Devices Conference (NMDC) | 978-1-6654-1892-8/21/$31.00 ©2021 IEEE | DOI: 10.1109/NMDC50713.2021.9677534

***Abstract*—Here we report on the design, synthesis and characterization of a stretchable strain sensor using a cracked multi-walled carbon nanotube film plotted on an elastomer sheet substrate. This bilayer sensor was developed for measuring strains at levels much higher than the conventional metallic foil-based strain gauges; while achieving higher gauge factor, lower hysteresis and improved linearity comparing to other current advanced flexible strain sensors. Such improved piezoresistive responses originate from reproducible opening and closing of the uniformly distributed, high density microcracks that were generated in the carbon nanotube thin film during controlled pre-stretch training. The constraining of microcrack opening-and-closing and nanotube rotation help to stabilize and mitigate large strains and significant resistance variation, leading to superior mechano-electric performances.**

Keywords — Flexible strain sensor, cracked film, carbon nanotube film, plotting.

I. INTRODUCTION

Sensing and actuating devices are rapidly evolving beyond traditional industrial machinery applications. They began to penetrate into our daily life at an accelerated pace, as the miniaturization and multi-functionality of such devices quickly progressed. Most sensors transduce external stimuli into electrical signals for easier quantification and processing over other types of characteristic information. The conversion of signals can be accomplished either through physical or chemical processes, with physical sensors being more widely developed and adopted mostly due to practicality [1]. In developing new devices and capabilities for personal health/recovery monitoring, on demand treatment, human-machine interface and prosthesis/ enhancement [3] – [4], needs for non-traditional sensing materials and structures with compatible mechanical and electrical properties are rising. Conventional metallic and ceramic materials often lack the compliances, flexibility and stretchability needed for these applications; new materials and corresponding fabrication technologies are needed [2]. For example, traditional resistive or capacitive based stress sensors/strain gauges mostly have their measurement range limited below 5% strain [5]. To sustain strains desired for flexible applications, "soft" substances are needed. A common practice of developing strain sensitive soft devices is to incorporate nano/micro functional materials with highly ductile stretchable polymers to obtain enhanced sensitivity, working range and durability far exceeding the performances of the individual constituent materials. Functional materials that have been explored include: metal nanowires, nanofibers, nanoparticles, carbon-based nanostructures (carbon black, carbon nanotube and graphene), and ionic liquids [6]. Among these, carbon nanotubes (CNTs) stand out due to their outstanding electrical, thermal and mechanical properties and high chemical stability[7]–[9]. Applications of CNTs have been explored in many microstructural forms including composites [10], thin films [11], forests and sponges [12]. Their electrical conduction mechanism and its dependence on physical deformation are different from those of traditional uniform materials and can exhibit "extraordinary" piezoelectric behavior. [13]. For conventional materials and structures, the electrical conductivity can generally be considered as an intrinsic physical parameter and exhibit weak dependence on the environment. But for highly non-uniform structures such as the interacting nanomaterial-polymer systems, the nanostructure distribution, inter-material charge transport, geometric deformation and defect structure will all significantly affect the mechano-electric responses. Understanding and control of the microstructure and its evolution during deformation in such material systems will be of critical importance in developing reproducible and reliable soft devices.

978-1-6654-1892-8/21/$31.00 ©2021 IEEE

In this paper , we report on the synthesis and characterization of cracked multi-walled (MW) CNT films formed on a rubber substrate for soft strain sensor applications. MWCNT thin films were first plotted on elastomer sheets from an aqueous suspension in rectangular patterns and microcracks (with certain density and average individual crack length) were then set in the CNT layer after the bilayer material system was subjected to a pre-stretch training process. In such bonded cracked CNT structures, strain in the CNT layer is mostly accommodated by nanotube rotation and separation and the electrical conductivity of the CNT layer will be significantly affected by micro-crack opening and closing. These strain sensors exhibit high cyclic repeatability, large gauge factor, small hysteresis and improved linearity.

II. EXPERIMENTAL

A. Materials

Multi-wall carbon nanotubes (MWCNT, NC7000 series) used in this study were purchased from Nanocyl, Belgium, with an average diameter of ~9.5 nm and a length of 1.5 µm. Sodium dodecyl sulfate (SDS) powder, purchased from Sigma Aldrich was used to synthesize a stable and homogeneous aqueous MWCNT suspension. Neoprene rubber sheets (1/32" thickness) from McMaster-Carr were used as elastomer substrates.

B. Sensor fabrication and characterization

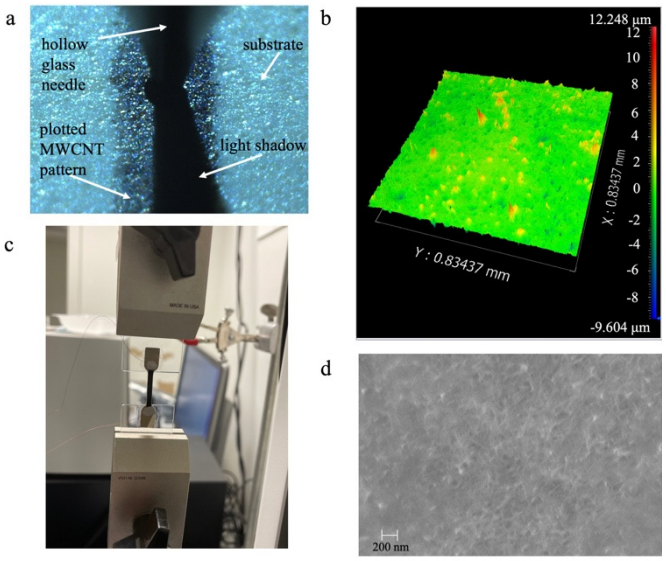

Fig. 1. (a) MWCNT solution plotted on substrate using SonoPlot Microplotter II (b) Optical profilometer measurement of substrate (c) Strain sensor test setup (d) SEM image of microstructure MWCNTs thin film

SDS powder was first dissolved in distilled water and magnetically stirred for 12 hours at room temperature to form a 1.2 wt% SDS solution. Multi-wall carbon nanotubes were then added into the as-prepared SDS solution to form a 0.9 wt% suspension. A probe-type sonicator was used to homogenize the CNTs (typical ultrasonication time is 7 hours) in solution. The obtained suspension was then used as ink for continuous fluid stream plotting on top of the commercial Neoprene rubber sheet.

The fabrication and basic characterization of the flexible strain sensors are illustrated in Figure 1. First, the Neoprene rubber sheet samples were cleaned in DI water and then in ethanol with sonication for 20 minutes. MWCNT thin films in a rectangular shape (typical size: 25 mm by 2 mm) were plotted on to the rubber sheet using a SonoPlot Microplotter II. The Microplotter functions using capillary force to collect and resonant vibrations to dispense solution from a glass capillary needle. The tip opening of the hollow capillary needle used in this study has an 80 µm diameter. The needle was set to move in the x-y plane, parallel to the printing surface, at a speed of 1 mm/s in each motor direction. Trace width of the plot is about 80-100 µm and the step distance was set to be 50 µm, plotting a 25 mm by 2 mm pattern, consumed about 0.785 mm^3 suspension. Patterned MWCNT films were then dried atmospherically and the rubber sheets were cut into desired size and shape (with CNT films being part of the structure) for characterization or application. MWCNTs film thickness and structure are dependent on not only CNT sizes and suspension concentration, but also capillary needle size, needle tip-substrate separation distance, needle motion speed/direction and plotting repeats. Figure 1(a) is an optical snapshot of the capillary needle and sample during plotting. A 3D optical profilometer measurement (ZeGage™ Pro) was used to evaluate the surface morphology of a MWCNT film on rubber substrate. As shown in Figure 1(b), in this representative area of 0.83 × 0.83 mm^2, the plotted MWCNT film has a relatively smooth surface with typical surface height variation within 4 µm, indicated by the majority of the profilometer image being green or yellow in color. To reduce contact resistance and improve electrode stability during the large strain electrical measurements, two extended Au pads were sputter deposited at the two ends of the MWCNT thin film strip. Silver paste was then used to fix soft copper wires with 100 µm diameters to the Au pads as electrical leads for equipment connection. Two end portions of the dog-bone shaped sheet sample were then glued to two microscopic glass slides for sample clamping to avoiding direct mechanical contact with the Au/Ag pasted electrodes during testing. This electrode setup was shown to be able to improve contact resistance stability during measurement and reduce the possibility of premature connection failure. Scanning electron microscopy (SEM) has been used to study the microstructure of the CNT films. As show in Figure 1(d), for the estimated 300 nm thick CNT film, a uniform distributed network structure is formed with CNTs showing certain degrees of alignment. We believe this is due to the shear alignment during plotting process.

III. RESULTS AND DISCUSSION

To establish baselines for the electrical behaviors of the current strain sensing material and structure, the plotted MWCNT films were first characterized with no external load applied. Figure 2(a) shows the I-V measurements for three thin film samples with different thicknesses. Here the MWCNT thin film thickness are controlled by the number of repeated plots of the rectangular pattern on the substrate. With all other parameters kept same, the MWCNT film thickness can be

considered to be directly proportional to the number of plot repeats (No. of passes). All three samples exhibit Ohmic behavior in the ambient measurement condition. Resistances of the three samples are 10kΩ, 7 kΩ, and 3.5 kΩ for the 1, 2 and 3 plotting repeats respectively. With increasing MWCNTs film thickness, there is clear reduction in sample resistance and this close to linear dependence of conductance to film thickness is an indication of uniform microstructure with constant CNT-CNT junction density distribution in the plotted film.

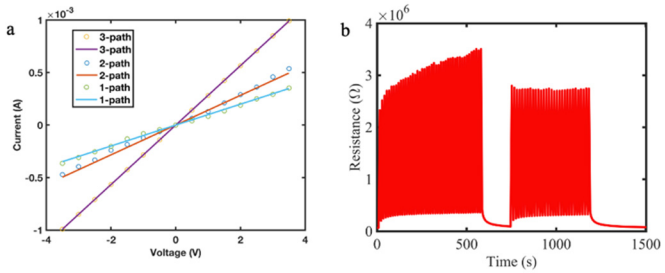

Fig. 2. (a) I-V curves of three plotted MWCNT films with different thicknesses, in the rest state (dot:measurement, line:fitting) (b) Sensor piezoresistive responses during training (35% maximum strain) and measurement (30% maximum strain) cycles

To evaluate the bilayer strain sensor performances, samples were clamped to a linear motorized force test stand (Mark-10, ESM301L), which is capable of testing under variable strain and variable strain rate conditions. Currents passing through the samples were measured under a constant potential voltage of 0.5 V with an electrochemical workstation (Autolab PGSTAT204). Figure 2(b) shows the piezoresitive responses of a MWCNT sensor sample with one layer plotting during initial "training" (40 cycles to 35% strain) and the follow up "measurement" (30% strain). There is a clear distinction in the sample piezoresitive responses during these two processes: during the initial training process, measured sensor resistance increases with continued cycling; whereas for the measurement phase cycles the sensor exhibits much more stable and reproducible response.

In order to explain this mechanoelectrical phenomenon, samples were mounted on a home-built picomotor driven stage and studied under an optical microscope. As shown in Figure 3(a), high density of microcracks emerged across the initially uniform MWCNTs thin film during training. These microcracks are uniformly distributed with the crack length direction perpendicular to the loading direction. Microcrack equilibrium configuration, including density and average crack length, are determined by the maximum training strain. Training is the process for the MWCNT film to re-configure and form the microstructure that can accommodate deformation imposed by the supporting rubber substrate. After training, and during the measurement process, there is no new microcrack generation or crack length change as long as the strain does not go beyond the maximum training strain. Only the microcrack width will change according to external loading, as shown in Figure 3. Finite element simulation also showed that for the strongly coupled CNT/rubber bilayer, stress at the microcrack tip is largely alleviated, as shown in Figure 3(b). This serves to explain the stability of microcrack and thus the piezoresitive responses.

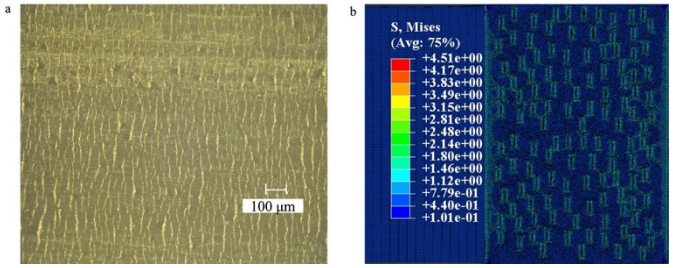

Fig. 3. (a) Optical plane view image of the MWCNT film on rubber when the applied tensile strain is 30% (b) Finite element simulation of the microcrack configuration in the CNT thin film on rubber layer at 30% strain

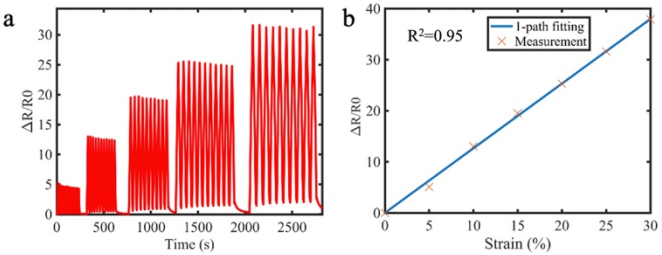

Fig. 4. (a) Cyclic piezoresistive responses of the sensor with increasing measurement strain ranges. (b) Current strain sensor has a linear resistance changes dependence on strain variation.

Samples were then tested under different strains to determine the gauge factor across the entire operating range. The gauge factor (relative change of resistance versus applied strain; GF = $\Delta R/R0*\varepsilon$) shown in Figure 4(a) was about 120 across the entire 0-30% strain range. Within the 30% strain measurement range, the resistance change increases linearly with strain ($R^2 \sim 0.95$) shown in Figure 4(b). This linearity is desirable for practical sensor application as nonlinearity adds complexity to calibration and data processing of the output signal. There are reports of crack-based strain sensors that can have a GF factor as high as several thousands, but those sensors often show poor linearity or have a very narrow linear response range [13]. Our MWCNT-rubber strain sensors possess high sensitivity and good linearity across the whole working strain range.

Another important characteristic of strain sensor performance is the hysteresis. For conventional metals, mechanical hysteresis is normally negligible. But viscoelasticity is intrinsically significant for polymeric materials and the hysteresis will be amplified by additional energy dissipation and relaxation when there are interactions among different materials. Hysteresis will affect strain sensor response time, accuracy and reliability. Current sensors have a thin film on thick elastomer a bilayer design and the elastomer properties will dominate the sensor hysteretic behavior. By choosing a highly elastic substrate, it is possible to minimize this hysteresis.

Such nanostructured sensor performances are very sensitive to the CNT and elastomer substrate selection, fabrication parameters and thus resulted sample microstructures. Individual sensor behavior is further defined and can be tuned through manipulating the microcrack configuration formed during training. It is found that using microplotting it is possible to generate reproducible CNT films providing the synthesis

parameters including capillary tube size, plotting speed and patterning directions are identical. To better understand the crack formation, growth and fatigue properties, we are currently carrying out further micromechanical/conductivity simulation and experimental crack measurement research to stablish quantitative model of the piezoresistive effect in such a nanostructure to improve the controllability and reproducibility of these sensors.

IV. CONCLUSION

In this work, we demonstrated a highly sensitive, microcrack based MWCNTs-rubber strain sensor which can be used to detect large mechanical strains. This sensor exhibits a large gauge factor value (around 120 up to 30%), a linear mechanoelectrical response and low degree of hysteresis that covered the full strain range. This excellent mechanoelectrical performance was carefully designed and achieved by the uniformly distributed microcracks across the whole MWCNTs thin film. In-situ optical microscope images clearly show an opening/closing of the microcracks during stretching/releasing process. The hydrophilicity and strong bonding between rubber substrate and MWCNTs thin film guaranteed a continuous and stable external load transfer from soft substrate to sensing materials during measurements. This strain sensor has great potential for applications in the fields of health-monitoring, human motion detection, soft robotics.

ACKNOWLEDGMENT

This research was supported in part by internal funding from the University of Houston.

REFERENCES

[1] L. Dai, Y. Wang, X. Zou, Z. Chen, H. Liu, and Y. Ni, "Ultrasensitive Physical, Bio, and Chemical Sensors Derived from 1-, 2-, and 3-D Nanocellulosic Materials," *Small*, vol. 16, no. 13, pp. 1–25, 2020, doi: 10.1002/smll.201906567.

[2] P. Cai, C. Wang, H. Gao, and X. Chen, "Mechanomaterials: A Rational Deployment of Forces and Geometries in Programming Functional Materials," *Adv. Mater.*, vol. 33, p. 2007977, 2021, doi: 10.1002/adma.202007977.

[3] M. Amjadi, K. U. Kyung, I. Park, and M. Sitti, "Stretchable, Skin-Mountable, and Wearable Strain Sensors and Their Potential Applications: A Review," *Adv. Funct. Mater.*, vol. 26, no. 11, pp. 1678–1698, 2016, doi: 10.1002/adfm.201504755.

[4] S. Huang, Y. Liu, Y. Zhao, Z. Ren, and C. F. Guo, "Flexible Electronics: Stretchable Electrodes and Their Future," *Adv. Funct. Mater.*, vol. 29, no. 6, pp. 1–15, 2019, doi: 10.1002/adfm.201805924.

[5] W. B. Dobie, P. C. G. Isaac, and G. O. Gale, "Electrical resistance strain gauges," *Nature*, vol. 154, no. 3898, p. 90, 1944, doi: 10.1119/1.1932512.

[6] L. Duan, D. R. D'hooge, and L. Cardon, "Recent progress on flexible and stretchable piezoresistive strain sensors: From design to application," *Prog. Mater. Sci.*, vol. 114, no. January 2018, p. 100617, 2020, doi: 10.1016/j.pmatsci.2019.100617.

[7] P. R. Bandaru, "Electrical properties and applications of carbon nanotube structures," *J. Nanosci. Nanotechnol.*, vol. 7, no. 4–5, pp. 1239–1267, 2007, doi: 10.1166/jnn.2007.307.

[8] S. Xie, W. Li, Z. Pan, B. Chang, and S. Lianfeng, "Mechanical and physical properties on carbon nanotube," *J. Phys. Chem. Solids*, vol. 61, no. 7, pp. 1153–1158, 2000, doi: 10.1016/S0022-3697(99)00376-5.

[9] A. M. Marconnet, M. A. Panzer, and K. E. Goodson, "Thermal conduction phenomena in carbon nanotubes and related nanostructured materials," *Rev. Mod. Phys.*, vol. 85, no. 3, pp. 1295–1326, 2013, doi: 10.1103/RevModPhys.85.1295.

[10] C. X. Liu and J. W. Choi, "Patterning conductive PDMS nanocomposite in an elastomer using microcontact printing," *J. Micromechanics Microengineering*, vol. 19, no. 8, 2009, doi: 10.1088/0960-1317/19/8/085019.

[11] T. Yamada *et al.*, "A stretchable carbon nanotube strain sensor for human-motion detection," *Nat. Nanotechnol.*, vol. 6, no. 5, pp. 296–301, 2011, doi: 10.1038/nnano.2011.36.

[12] S. Ryu *et al.*, "Extremely Elastic Wearable Carbon Nanotube Fiber Strain Sensor for Monitoring of Human Motion," *ACS Nano*, vol. 9, no. 6, pp. 5929–5936, 2015, doi: 10.1021/acsnano.5b00599.

[13] H. Souri *et al.*, "Wearable and Stretchable Strain Sensors: Materials, Sensing Mechanisms, and Applications," *Adv. Intell. Syst.*, vol. 2000039, p. 2000039, 2020, doi: 10.1002/aisy.202000039.